

Efficient plane extraction using normal estimation and RANSAC from 3D point cloud



Lina Yang^a, Yuchen Li^{*,a}, Xichun Li^b, Zuqiang Meng^a, Huiwu Luo^c

^a Guangxi University, Nanning 530004, PR China

^b Guangxi Normal University for Nationalities, Chongzuo 532200, PR China

^c Changsha Xinghen Intelligent Technology Co., Ltd., Changsha, Hunan Province 410100, PR China

ARTICLE INFO

Keywords:

Plane extraction
RANSAC
Angular clustering
PCA
Normal estimation

ABSTRACT

Indoor plane extraction on point cloud has always been a research hotspot, in which random sample consensus (RANSAC) is known as a common algorithm. However, impacted by numerous occluded objects in the interior scene, the point cloud generated by the sensors may be missed in part of the aircraft area. Moreover, the conventional RANSAC method will cause the plane being incorrectly extracted. In this study, an indoor plane detection method is proposed based on space decomposition and an optimized RANSAC algorithm. In this method, the weighted PCA method is exploited to estimate the normal vector from point cloud, then the angular clustering is employed to divide the interior space for obtaining the building components. Subsequently, an optimized RANSAC method is adopted to detect planes from the building components obtained. To be specific, the proposed RANSAC method selects the candidate points by using a heuristic search strategy, and then the mentioned candidate points are used to estimate the final plane. The proposed method can handle the overlapping patches that cannot be extracted by using the conventional RANSAC method. The proposed method is assessed on 4 indoor datasets. As indicated by the experimental results, the proposed method can detect the plane structure efficiently and effectively.

1. Introduction

Three-dimensional (3D) scene understanding has always been a research hotspot in the field of robot vision [1]. By employing various 3D sensors (e.g., LiDAR and depth camera), the robot is capable of analyzing the captured scene effectively in real time. Therefore, related image processing technologies are used in many fields to assist its development and innovation [2–4]. To be specific, the extraction and modeling of indoor 3D point cloud objects is found as a hotspot in existing research. On the whole, the interior scene environment is more complicated, and the scanned point cloud data are more disordered. Thus, considerable objects are blocking each other and cannot be modeled automatically. The complex indoor point cloud should be segmented, and each simple geometry should be formed [5]. Through the identification and modelling of the mentioned elements, the complex 3D model of interior scene is finally built.

Existing research reported that most of man-made environment and objects are composed of multiple plane areas. The plane is capable of

structurally describe the corresponding scene and shows the target or clue to perform specific tasks in some cases (e.g., target extraction, real-time location and map construction (SLAM), as well as indoor scene reconstruction) [6]. Plane extraction is considered a vital stage in the understanding of 3D scene. The plane, one of the basic geometry elements, can be defined by using mathematical models, so the model-based fitting method can be a typical method for plane extraction. To be specific, Random Sample Consensus (RANSAC) and Hough transform (HT) are the two methods applied most commonly. The RANSAC algorithm exhibits better performance compared with HT for accuracy and speed of the extraction results. Furthermore, Region Growing is also a widely used method, but in the growth process, the growth parameters are more sensitive to noise.

Based on the idea of pre-clustering, this study proposes an algorithm to extract the main planes of interior space (e.g., walls and floors). The algorithm falls into two stages. First, a robust normal vector estimation algorithm is adopted to calculate the normal vector of the internal point cloud. The space is divided by complying with the similarity of the

* Corresponding author.

E-mail addresses: lnyang@gxu.edu.cn (L. Yang), 18406504901@163.com (Y. Li), lixichun@gxun.edu.cn (X. Li), mengzuqiang@163.com (Z. Meng), luohuiwu@gmail.com (H. Luo).

normal vector. Subsequently, an optimized RANSAC algorithm is used to estimate the plane parameters of the acquired component subset for achieving the final result. As indicated by the experimental Results, the plane detection algorithm proposed in this study can reduce the noise data interference in the plane detection work. Moreover, in the RANSAC algorithm, two thresholds were set to detect the horizontal distance and normal distance between points, respectively, to successfully extract the adjacent overlapping planes in the space.

The arrangement of this study is presented below. First, the main plane detection algorithms are reviewed in the second section. In [Section 3](#), the proposed plane detection method for interior space is described, in which [Section 3.1](#) describes the process of space decomposition and the [Section 3.2](#) explains the proposed RANSAC method. In [Section 4](#), the case study of this study and the assessment results of the method are presented. Lastly, the conclusions are drawn, which involve the description of the major advantages of the proposed method, the defects of the experiment and the areas for improvement.

2. Related work

On the whole, image processing is required to achieve the final technical task in robot vision technologies [7], and other applications based on image processing are also very extensive [8,9]. Some encryption technologies [10], intelligent industries [11] and so on will use image processing for auxiliary development. Using 3D point cloud processing to detect build-up environment has been an active task. In a range of fields (e.g., ground detection, obstacle detection and building reconstruction) the plane should be detected in the point cloud. Plane detection can be recognized as the basic technology of 3D scene understanding, as well as a vital part of it. Impacted by the sophisticated environment of the indoor scene, researchers have been committed to the research of the problem of plane detection in indoor scenes. The research technology can fall into two types, i.e., conventional methods and deep learning methods. The conventional indoor scene plane detection method is detected through predefined model features without supervision, and the depth learning method is achieved by learning the features from training samples.

Mainly three types of plane estimation methods are included in conventional methods, i.e., Random Sample Consensus (RANSAC) method, region growing method, as well as Hough transform (HT) method. For the Region Growing method [6] the local features extracted from the domain of each point is used to continuously merge the regions with similar attributes, and a complete planar region is finally generated. Leng and Xiao [12] developed a cache-octree region growing (CORG) algorithm, which can achieve the growth of the region under the shortest distance from the point to the least square plane that is composed of the point and the region. Moreover, the generated region always achieves the minimal plane fitting error rate, till the region cannot add novel points. The KNN search method is adopted to build the cache octree and retrieve the nearest neighbor of a point. However, this method is only dependent of the distance information of points, and the problem of over-extraction may exist. Several hybrid methods combined with various geometric information have been tried to increase the accuracy of plane segmentation. Khaloo and Lattanzi [13] classified 3D points into edge points, boundary points and surfaces. Boundary points and edge points are adopted to stop the growth of the region, and then the region grows according to the surface normal similarity. This method applies to scenes with significant boundary features. If the edge of the plane is blurred, the extraction may fail. Rabbani and Heuvel [14]

proposed a region growing technique based on smoothing constraints, which was used to extract smoothly connected regions from unstructured 3D point clouds. This method applies the normal vector of the surface and the approximate local curvature as the measure of local geometry to determine the respective segment, whereas it is vulnerable to noise and sharp features in the point cloud model. In [15], the above method was used to automatically extract 3D point cloud data corresponding to the pipes of the industrial plant. In this work, the target 3D scans data had relatively low noise, and there was no challenge of data loss under occlusion or significant variations in surface roughness and curvature. Dimitrov and Golparvar-Fard [16] employed multi-scale feature extraction (e.g., the roughness and curvature of the respective 3D point) to introduce a region-growing segmentation for building point clouds.

Hough transform (HT) and RANSAC method can be recognized as a region growing method, with the aim to gather points with the identical attributes in the same plane model. The point cloud data exhibit better geometric characteristics, the use of mathematical models can more effectively describe the scene. The core idea of HT is to map the input samples to several feature spaces, then vote in the accumulator, and select the accumulator unit with the most votes as the model parameters. Plane detection requires a 3D accumulator defined by the plane normal and the distance from the plane to the origin. When there are considerable data fitting models, the Standard HT (STH) [17] encounters the problems of sensitivity to accumulator design and complex computation, and it cannot ensure that all planes can be detected. Leng and Xiao [18] proposed a technique combining region growing and Hough transform for optimization. The plane clusters generated by HT act as the growth unit, and the region growing is achieved by judging the normal and curvature similarity of the plane clusters. However, this method only applies to point cloud scenes with uniform density; otherwise, the potential plane cannot be detected. Limberger [19] extended the method proposed by kernel-based HT (KHT) and proposed a clustering technique by exploiting on approximately coplanar samples to optimize the voting process. This method was applied for the plane detection of large-scale unorganized point clouds. Vera and Lucio [20] developed a real-time Hough transform method based on implicit Quad-tree. With an effective Hough transform voting scheme, the uncertainty of the optimal fitting plane of the respective planar cluster was modeled as a ternary Gaussian distribution, so the cluster detection was achieved. Over the past few years, the method based on deep learning has been extensively adopted to extract the plane [21,22]. However, the mentioned methods should be trained on custom datasets.

Random sample consensus (RANSAC) [23] is another popular 3D shape detection technique. Compared with Hough transform technology, the result obtained by RANSAC algorithm is more successful and rapid (Tarsha-Kurdi and Landes [24]). In addition, the RANSAC algorithm is more robust (Gallo and Manduchi [25]). Since it initially emerges in computer vision, the algorithm of computer vision has been optimized significantly. Accordingly, in this study, RANSAC algorithm is selected as the method of plane extraction of interior space, to assess and improve its results. The typical RANSAC plane extraction method is to repeatedly fit a hypothetical plane to a set of 3D data points and maximize the number of inliers. The defect of this method is that the extraction will fail when there are multiple planes interspersed with each other in the scene. In numerous cases, multiple planes will be inevitably stacked and crossed in complex scenes, and researchers have made corresponding optimizations in different scenarios. To be specific, the pre-clustering of the original data is a more popular idea, which

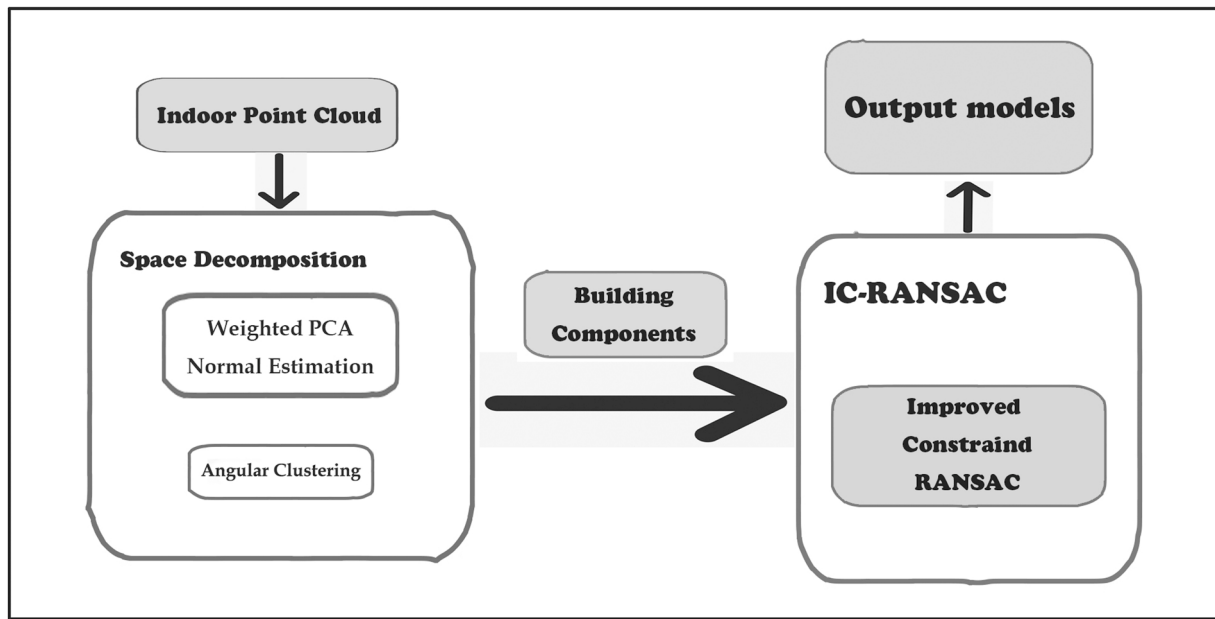


Fig. 1. General overview of the process.

avoids the disorderly selection of random data. Gallo and Manduchi [25] proposed the CC-RANSAC method, which assesses the fitness of the candidate plane by detecting the maximal connected component of the inliers in each iteration. This method is capable of achieving the simple detection problem of crossing the plane in the scene. Qian and Ye [26] further improved the cc-RANSAC method by adding normal vector information, each cluster is allowed to be estimated in clustering and fragment join steps, thereby optimizing the existing method. Marcelo and Saval-Calvo [27] chose to add scene knowledge at the clustering stage and RANSAC model fitting stage to optimize the results. In addition, there are some other ideas to improve RANSAC. Schnabel and Wahl [28] proposed an efficient point cloud shape detection algorithm, which is capable of dealing with large-scale point clouds. This algorithm can extract various original shapes, while retaining the high characteristics of RANSAC normal form (e.g., robustness, versatility and simplicity). Yuheng and Hao [29] summarized a wide range of RANSAC-based methods and summarized and compared them for robustness, accuracy and computing speed.

However, the RANSAC algorithm has the defect of extracting the continuous plane space into a single plane feature [30]. Thus, the parallel planes in the interior space may be extracted by RANSAC as part of the main plane (ground, wall). Thus, for the plane extraction of indoor scenes, conventional RANSAC shows significant limitations.

3. Methodology

This Section elucidates the proposed method. This method adopts the idea of pre-clustering, which primarily falls into two stages: decomposing the point cloud data of the indoor scene in an indoor space; using the variant RANSAC method to estimate the final plane model from the decomposed components. The overall research methodology is illustrated in Fig. 1.

3.1. Space decomposition

This section elucidates the space decomposition methods applied. Given the Manhattan-World hypothesis [31], most man-made objects comply with a natural Cartesian reference system. The assumption regarding interior space is that building components are primarily composed of horizontal components (e.g., floors and ceilings) and vertical components (e.g., walls and columns). In this study, the interior building components are aligned, in which the horizontal component is defined as the plane parallel to the x-y plane, and the vertical component is defined as the plane parallel to the x-z and y-z planes, respectively. Subsequently, the vertical structure and horizontal structure of the internal space are divided in accordance with the similarity of the normal vector. By using Manhattan-world, it is assumed that the original indoor point cloud is converted to the appropriate data format.

3.1.1. Normal estimation

Normal is a vital geometric feature in point cloud data model, so the normal vector estimation is a basic work in 3D point cloud processing. The principle component analysis (PCA) algorithm proposed by Hoppe and DeRose [32] has been extensively applied in normal vector estimation for its simple implementation. However, when obtaining point cloud data, impacted by equipment accuracy, scanning environment and external interference, the original data inevitably contain several defects or deviation points [33]. The mentioned noisy points may cause some errors in the estimation of the normal vector of the original point cloud. In particular, the normal vector at the edge point will have a significant error, which will cause mis-division in the subsequent spatial decomposition and will prolong the unnecessary calculation time. Accordingly, a weighted PCA algorithm is adopted to establish spatial distance constraints in the local neighborhood of sampling points, and weight functions are introduced for constructing the covariance matrix to suppress the effect of noise and improve the robustness of normal vector calculation of edge points or sharp points.

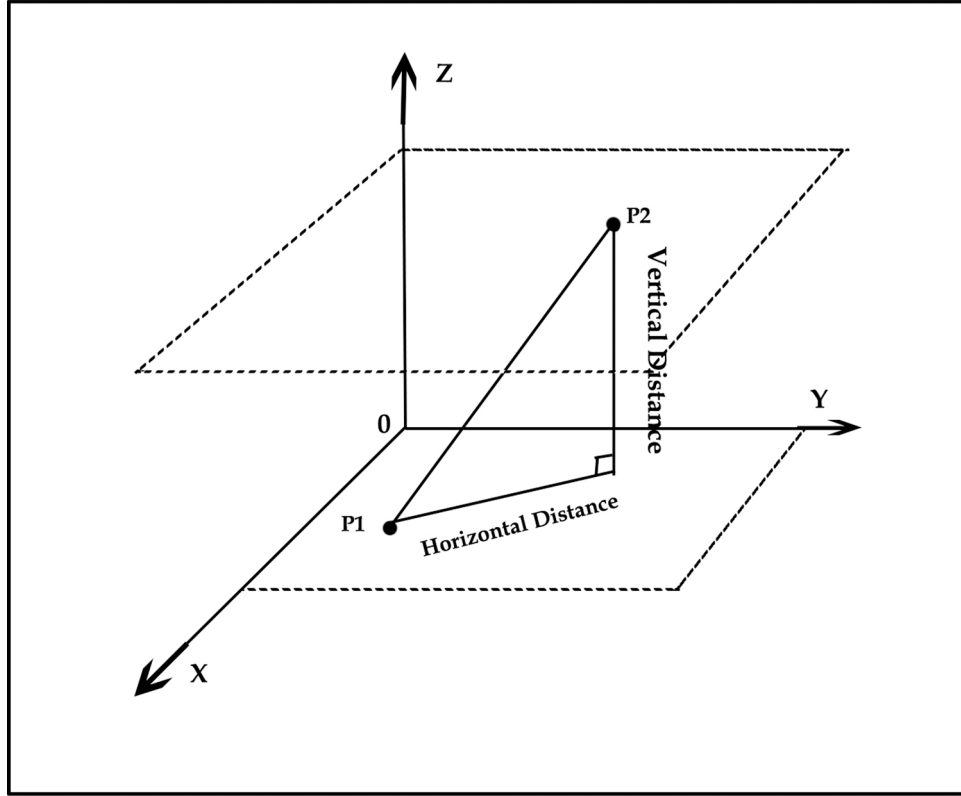


Fig. 2. Horizontal distance and normal distance between two points on two parallel planes.

The idea of the normal vector estimation is: we firstly select a sampling point $\mathbf{p}_i(x, y, z)$ and its K local neighbor points $\mathcal{N}_k = \{\mathbf{p}_k\}, k = 1, \dots, K$, then we use the least square principle to fit a local plane. Therefore, the normal \mathbf{n}_i of this plane is the normal of \mathcal{N}_k . The aim of least square plane is to minimize the total distance of \mathcal{N}_k to $\{\mathbf{p}_i\}$. We define our problem as follows:

$$\min_{\|\mathbf{n}\|=1} \sum_k^K ((\mathbf{p}_k - \tilde{\mathbf{p}})^T \mathbf{n})^2 \quad (1)$$

where $\tilde{\mathbf{p}} = \frac{1}{K} \sum_{k=1}^K \mathbf{p}_k$ is the center of the neighbors of \mathbf{p}_i .

The selection of neighborhood size will affect the uniformity of plane normal direction. For a large neighborhood, normals are smooth (for example, all normals on a planar point in the same direction), but the edges of objects are also smooth, so they are not so descriptive. In contrast, if the neighborhood is small, the normal is more affected by noise, and for a single plane surface, the normal do not very uniform. The traditional PCA method will cause the error of the normal at the edge, so we adjust the influence of the nearest neighbor points on the sampling points by adding distance constraints. We use the Euclidian distance (ED) to define the distance between the point to its neighbors:

$$D_k = \| \mathbf{p}_k - \tilde{\mathbf{p}} \|_2 \quad (2)$$

where \mathbf{p}_k is the sample point and $\tilde{\mathbf{p}}$ is the center of its neighbors. Now we take the adjacent points within the range of threshold ρ as consideration. The points outside the range of threshold are given different weights according to the distance. Because the farther away from the sampling point, the smaller the impact on the sampling point, reducing the allocation of its corresponding weight:

$$w_k = \begin{cases} 1 & D_k \leq \rho \\ \exp(-D_k^2/\tilde{D}_i^2) & D_k > \rho \end{cases} \quad (3)$$

Where \tilde{D}_i is the average distance from the sampling point to each neighboring point, and ρ the maximum distance from \mathbf{p}_i to the local plane fitted by its K nearest neighbors. The fitting problem of (1) now becomes:

$$\min_{\|\mathbf{n}\|=1} \sum_{k=1}^K w_k ((\mathbf{p}_k - \tilde{\mathbf{p}})^T \mathbf{n})^2 \quad (4)$$

We define a weight matrix \mathbf{W} with the diagonal elements to be the weight value of w_k :

$$\text{Diag}(\mathbf{W}) = \mathbf{I} \odot (\mathbf{W} \mathbf{1}^T) \quad (5)$$

where \odot is the Hadamard product. For the vectors weights w_i of \mathbf{W} associated with the neighbors, we define a weighted version of covariance matrix as follows:

$$\mathbf{M}_w = \frac{1}{\sum_1^K w_k} (\mathbf{p}_i - \tilde{\mathbf{p}})^T \text{Diag}(\mathbf{W}) (\mathbf{p}_i - \tilde{\mathbf{p}}) \quad (6)$$

Note that \mathbf{M} describes the local geometric information. The standard eigenvalue equation can be solved using singular value decomposition (SVD). The solution is given by:

$$\mathbf{M}_w \mathbf{V} = \lambda \mathbf{V} \quad (7)$$

where \mathbf{V} is the matrix of eigenvectors (principle components), and λ is the corresponding eigenvalues represented as diagonal elements, respectively.

In our case, the estimated normal vector is bidirectional, so the direction needs to be redirected:

$$\hat{\mathbf{n}}_i = \begin{cases} \mathbf{n}_i & \mathbf{n}_i(\mathbf{p}_i - \tilde{\mathbf{p}}) > 0 \\ -\mathbf{n}_i & \text{others} \end{cases} \quad (8)$$

The covariance matrix \mathbf{M}_w not only suppress the noise through different

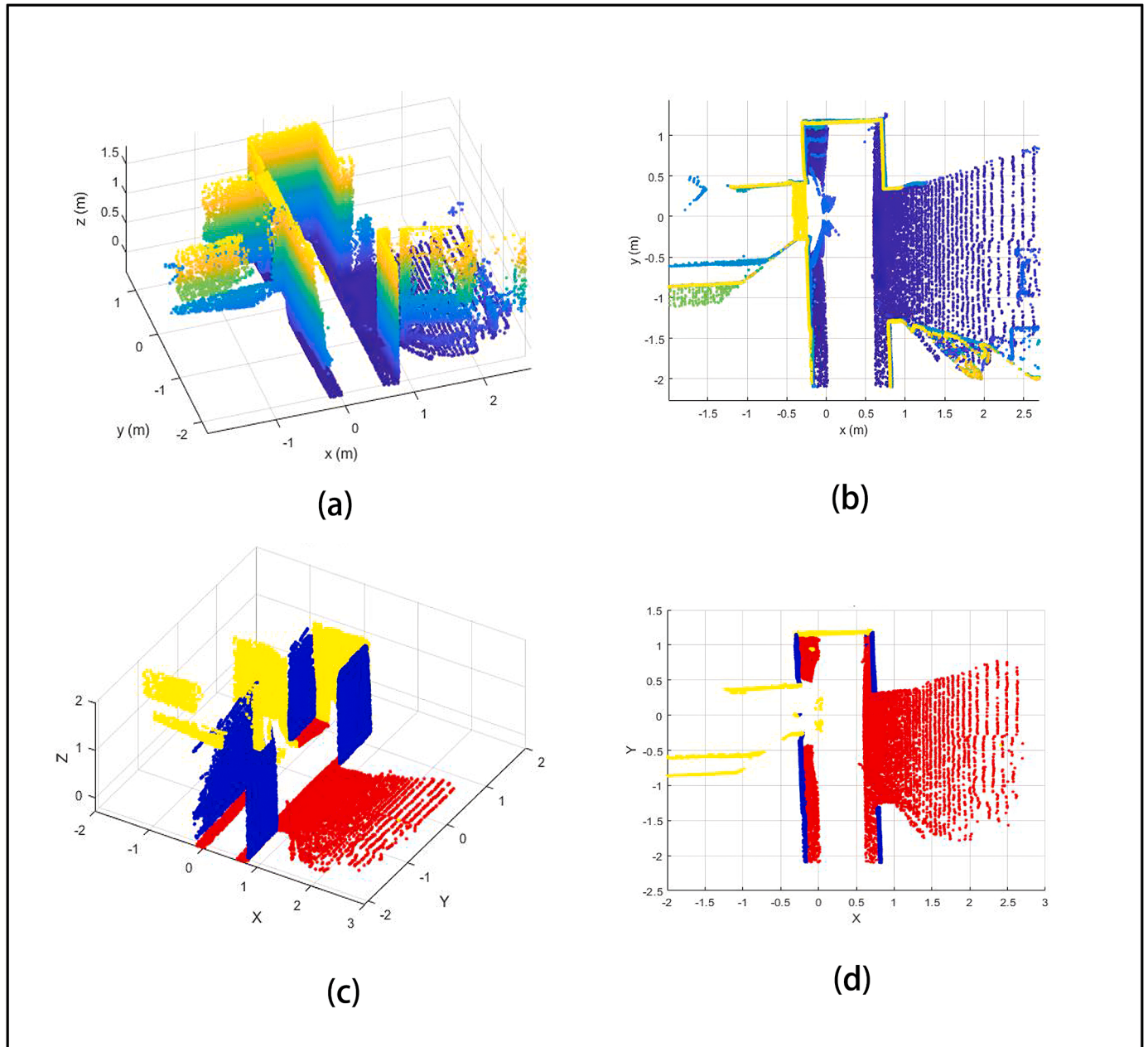


Fig. 3. Hallway.(a) and (b) are the side and top views of the Raw point cloud data of the hallway, respectively. (c) and (d) show the detection results of the main plane components of hallway, including four walls in yellow and blue, and the red in floor. (For interpretation of the references to colour in this figure legend, the reader is referred to the web version of this article.)

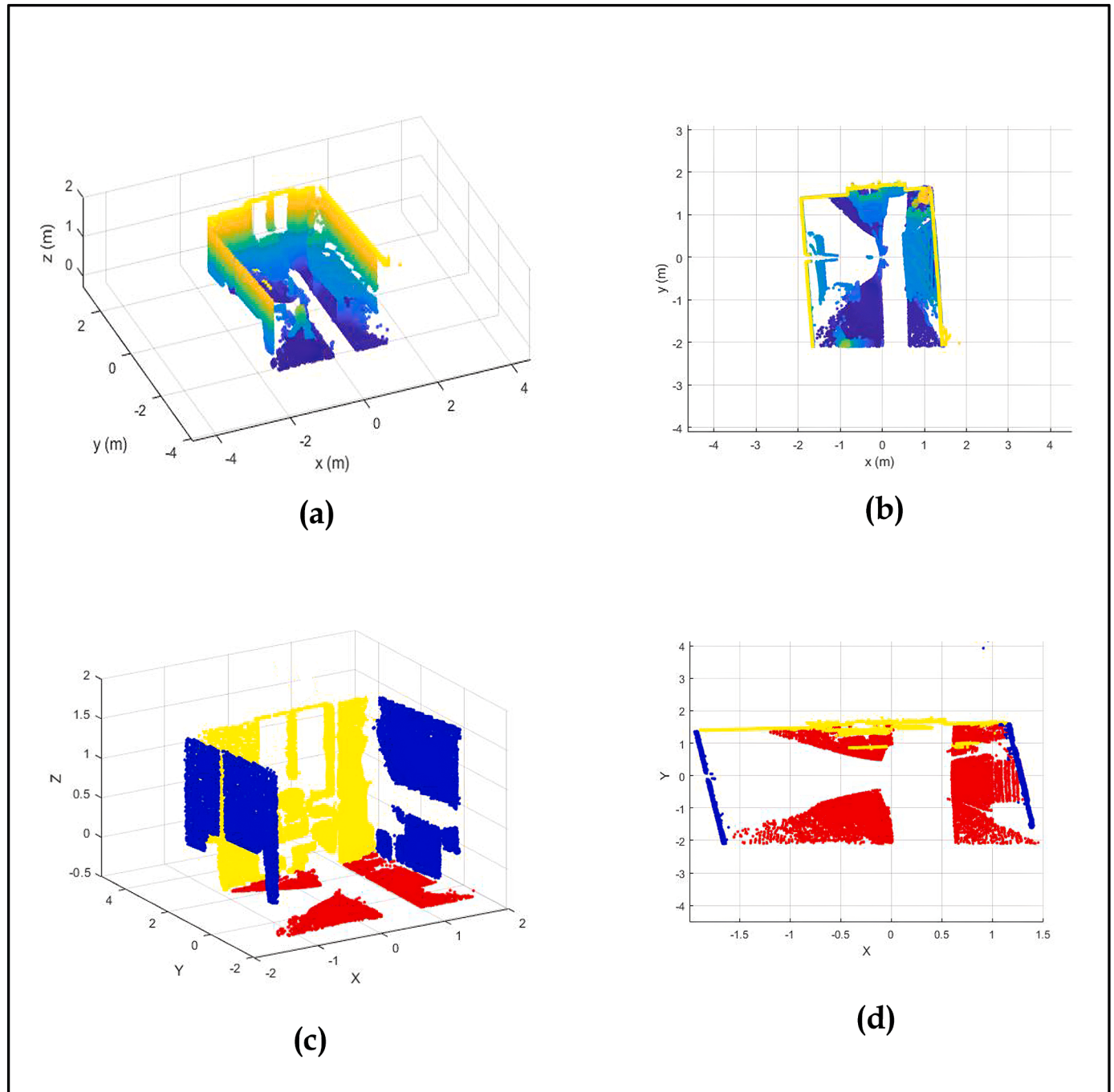


Fig. 4. Office1. (a) and (b) are the side and top views of the Raw point cloud data of the office, respectively. (c) and (d) show the detection results of the main plane components of office, including four walls in yellow and blue, and the red in floor. (For interpretation of the references to colour in this figure legend, the reader is referred to the web version of this article.)

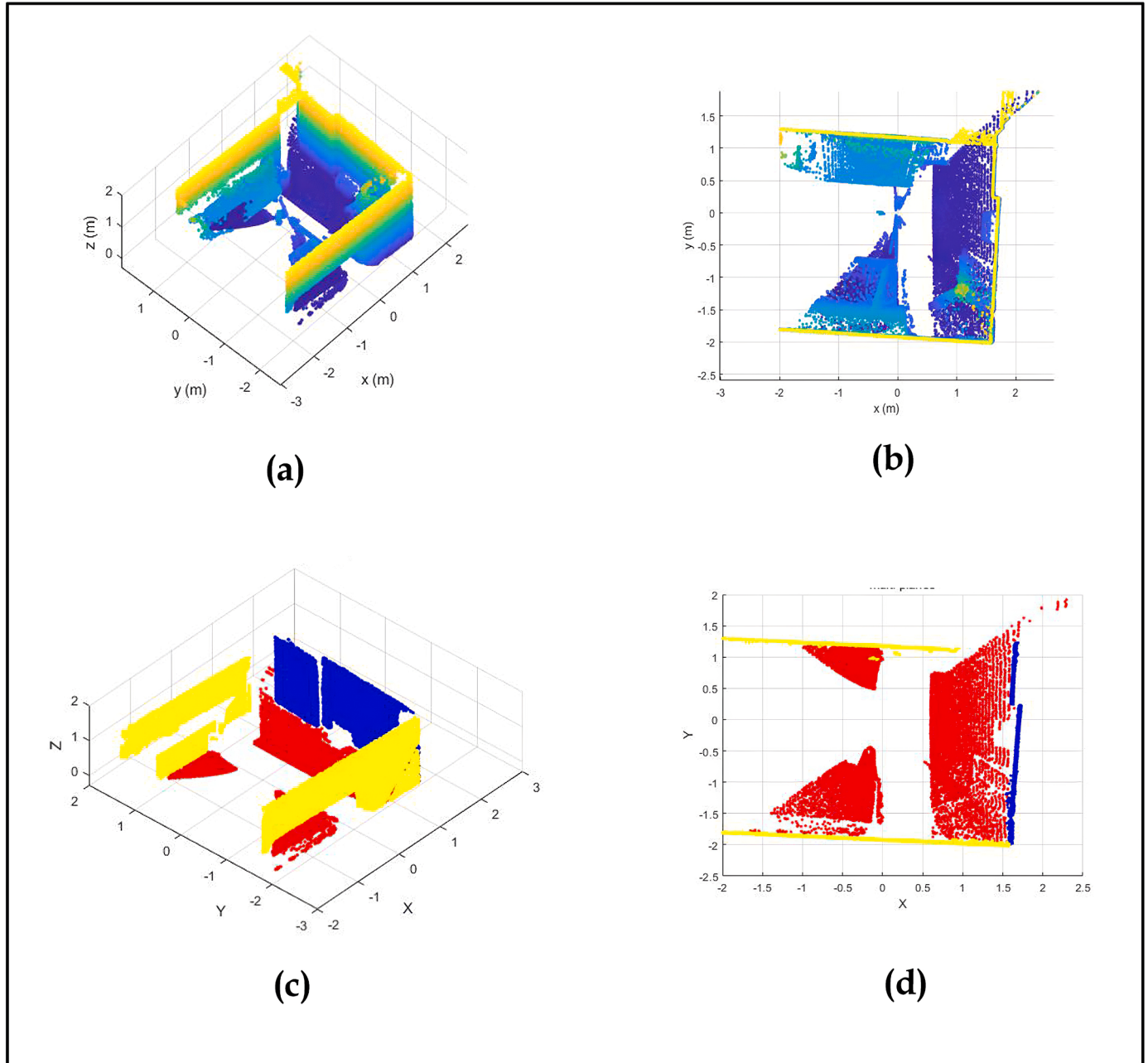


Fig. 5. Office2. (a) and (b) are the side and top views of the Raw point cloud data of the office, respectively. (c) and (d) show the detection results of the main plane components of office, including four walls in yellow and blue, and the red in floor. (For interpretation of the references to colour in this figure legend, the reader is referred to the web version of this article.)

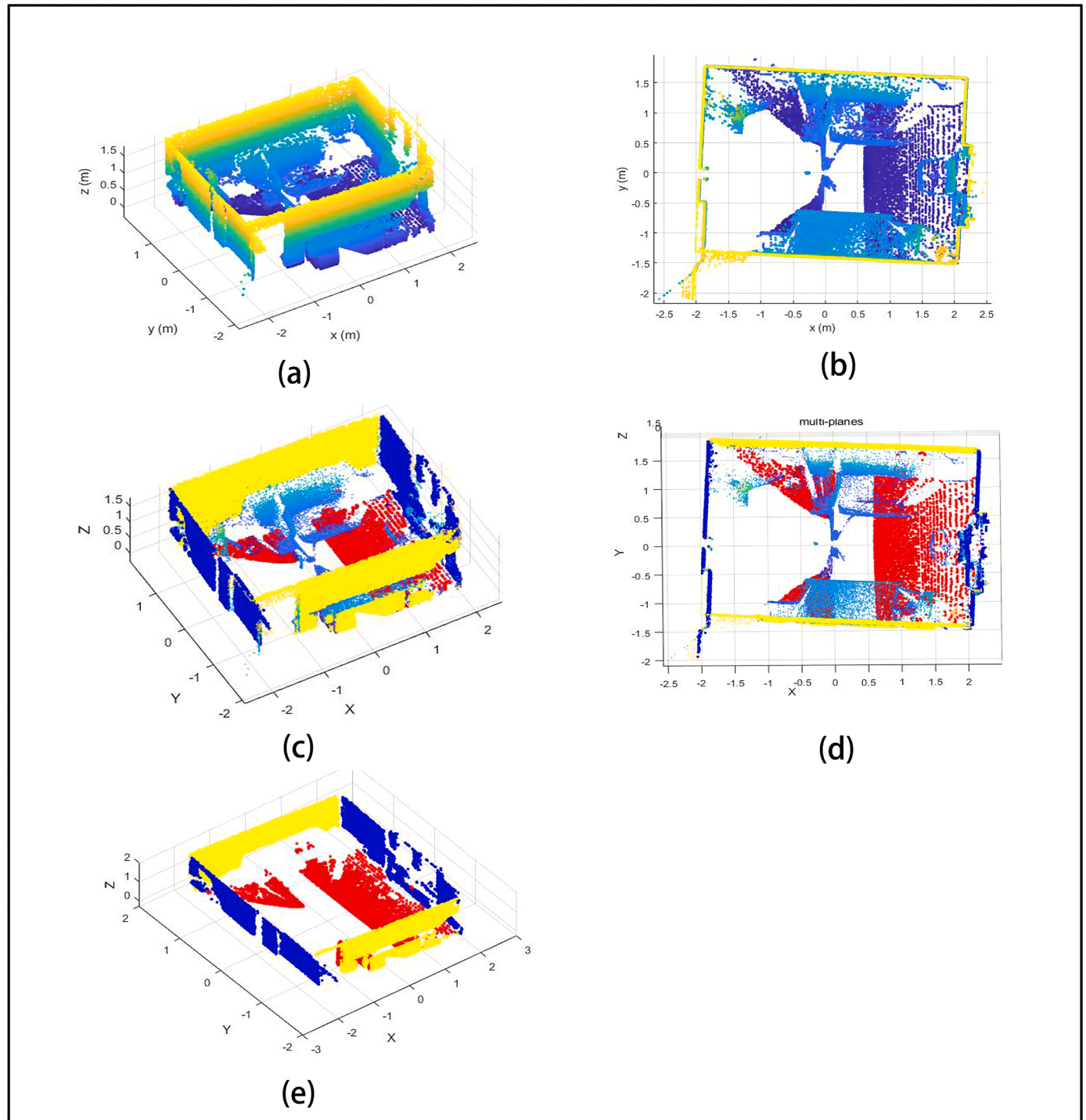


Fig. 6. Office3. The results include other indoor items.

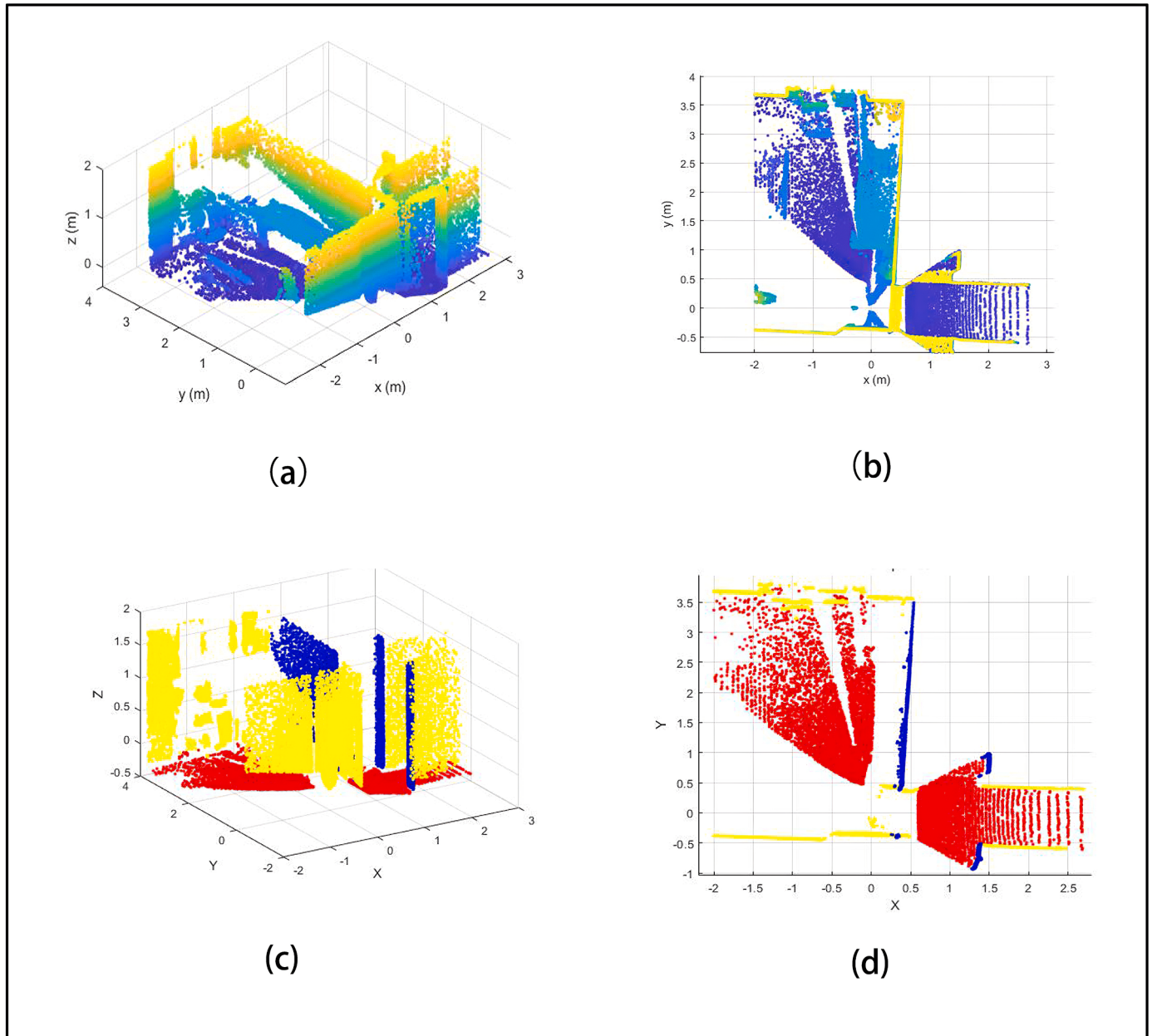


Fig. 7. Bathroom. (a) and (b) are the side and top views of the Raw point cloud data of the bathroom, respectively. (c) and (d) show the detection results of the main plane components of bathroom, including four walls in yellow and blue, and the red in floor. (For interpretation of the references to colour in this figure legend, the reader is referred to the web version of this article.)

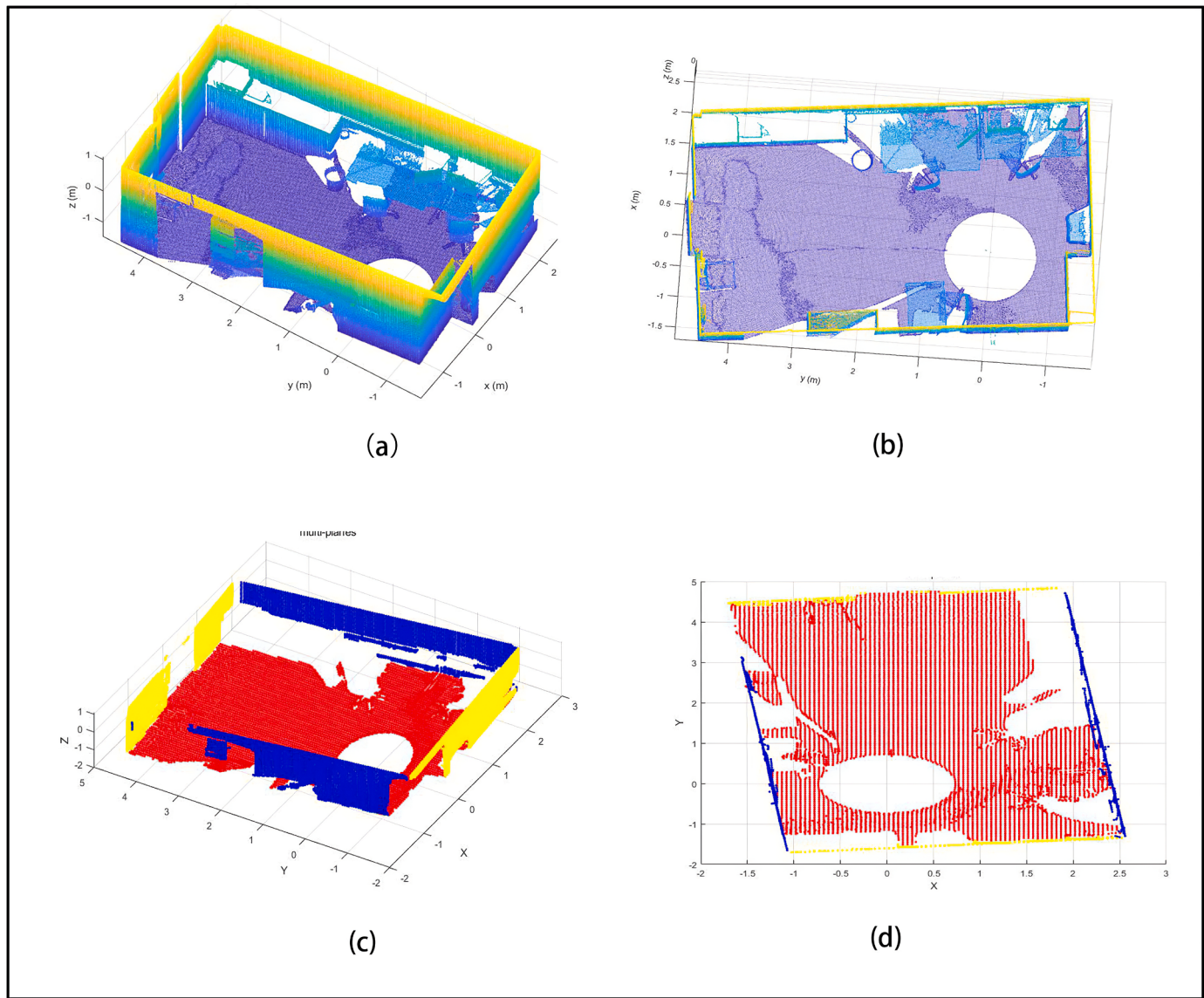


Fig. 8. Office room at UZH. (a) and (b) are the side and top views of the Raw point cloud data of the office, respectively. (c) and (d) show the detection results of the main plane components of office, including four walls in yellow and blue, and the red in floor. (For interpretation of the references to colour in this figure legend, the reader is referred to the web version of this article.)

Table 1
Parameters of the planes in the point cloud of Hallway.

Name	Parameter A	Parameter B	Parameter C	Parameter D
plane 1	-0.0117	-0.0077	0.9999	0.2492
plane 2	0.0698	-0.9976	0.0032	0.4319
plane 3	0.9992	0.0349	0.0178	0.2419
plane 4	-0.0314	0.9995	0.0098	-1.1693
plane 5	-0.9993	-0.03414	-0.0216	0.7615
plane 6	0.0827	-0.9965	-0.0081	-0.2374

weights, but also consider the influence of the distance of the neighborhood points on the sampling points. So the vector can be calculated accurately at the sharp edge.

3.1.2. Angular clustering

The normal vectors of two points pertaining to the identical plane or parallel separation planes are similar. Thus, an angular clustering

Table 2
Parameters of the planes in the point cloud of Office 1.

Name	Parameter A	Parameter B	Parameter C	Parameter D
plane 1	-0.0139	-0.0079	0.9999	0.2520
plane 2	-0.0863	0.9963	3.8132	-1.5420
plane 3	0.0681	-0.9964	0.0507	0.8786
plane 4	0.9969	0.0783	0.0128	-1.2914
plane 5	-0.9967	-0.0795	-0.0168	-1.7939

algorithm is adopted to get an initial clustering considering spatial position and direction for space decomposition.

For the calculated normal vector \mathbf{n}_i , the similarity of two normal vectors \mathbf{n}_1 and \mathbf{n}_2 is judged by calculating the angle between them:

$$\theta = \cos^{-1}(\mathbf{n}_1 \cdot \mathbf{n}_2) \quad (9)$$

The algorithm here is briefly summarized in Algorithm 1:

Algorithm 1. Angular Clustering

Input: the point cloud $PC = \{p_i|i = 1 \dots p\}$ and the normal vector of each point $N = \{n_i|i = 1 \dots p\}$
Output: vertical components C_v and horizontal components C_h

1. Create lists C_h to store clusters of horizontal components
2. Create lists C_v to store clusters of vertical components
3. for i:=< Num_{PC}
4. for the normal vector in each clusters
5. Calculate the angle θ_v between normal vector N_i and the normal vector of XY-plane with equation (9)

$$\theta_v = \cos^{-1}(\mathbf{n}_i \cdot \mathbf{n}_{xy})$$
6. if $\theta_v < \Delta\theta$
7. Add point into C_v
8. break
9. end if
10. end for
11. Calculate the angle θ_h

$$\theta_h = \cos^{-1}(\mathbf{n}_i \cdot \mathbf{n}_{xz})$$
12. if $\theta_h < \Delta\theta$
13. Add point into C_h
14. end if
15. end for
16. return C_v, C_h

Table 3
Parameters of the planes in the point cloud of Office 2.

Name	Parameter A	Parameter B	Parameter C	Parameter D
plane 1	-0.0209	-0.0071	0.9998	0.2500
plane 2	0.0643	0.9979	0.0060	-1.1740
plane 3	-0.0618	-0.9981	-0.0059	-1.9091
plane 4	1.0000	-0.0044	-0.0045	-1.6506
plane 5	-0.9983	-0.0078	-0.0576	-0.0168

Table 4
Parameters of the planes in the point cloud of Bathroom.

Name	Parameter A	Parameter B	Parameter C	Parameter D
plane 1	-0.0082	0.0091	0.9999	0.2430
plane 2	0.0547	0.9981	0.0272	0.3434
plane 3	0.0491	-0.9980	-0.0401	0.3588
plane 4	0.9984	-0.0547	0.0114	-0.3677
plane 5	-0.9984	-0.0461	0.0221	-0.0371

Table 5
Results for the Data at ETH.

Room	The Improved RANSAC		RANSAC	
	S_Dbw	Sp	S_Dbw	Sp
Hallway	0.5782	2	0.7582	1.1101
Office1	0.4939	1.9626	0.8007	1.8643
Office2	0.3742	1.8773	0.3941	1.7962
Bathroom	0.4600	1.4623	0.8195	1.4526

After angular clustering, we will obtain the corresponding subsets of horizontal and vertical components, and there will be multiple parallel planes in each subset. The next step is to separate the points of other indoor objects from the ground and the wall, and obtain the parameters of the floor and the plane of the wall.

3.2. Plane extraction

In this section, we propose an optimized RANSAC algorithm to estimate the main plane components (floor, wall) of the interior space, and separate other indoor objects from it. The conventional RANSAC algorithm is to iteratively calculate the final plane by randomly selecting three points in the point cloud. This is not targeted, and will increase the scale of computing. Accordingly, constructing a good candidate plane during random sampling can significantly reduce the running time and will not adversely affect the vector estimation. The algorithm mainly has two steps: first, the candidate point set is selected as a priori knowledge to construct the initial plane by using heuristic search strategy from the acquired component subset, and whether the remaining data accords with the confidence of the interior point is evaluated.

The main task of the RANSAC algorithm to extract plane is presented below. Select a minimal random point subset \mathcal{P} and adopt to define the initial plane model equation. The adjacent points to \mathcal{P} are selected to verify whether the model parameters continue to apply to all the points of the current point set, until the appropriate number of interior points in the model. Subsequently, the model error rate is calculated to test whether it is the best model. Run this process iteratively until the optimal model is reached. We define the plane model as:

$$ax + by + cz + d = 0 \quad (10)$$

where (a, b, c) denotes the normal vector of the unit on the plane; d represents the distance from the origin of the coordinate to the plane

fitted.

A vital part of the RANSAC is the selection of the threshold for determining the inlier of plane model. On the one hand, too large and too small threshold will cause over-extraction and incomplete extraction of the plane. On the other hand, the discriminatory basis of the threshold will impact the extraction results of the plane. In conventional RANSAC, the threshold is set in accordance with the distance from the point to the plane, and all points that are less than the distance from the point to the plane will be extracted as plane feature points. However, the mentioned feature points will cover some outliers, thereby probably causing the inaccurate results of plane extraction. In addition, in the indoor space, there will be some problems (e.g., cartons, carpets and other small items stacked on the ground or leaning against the wall). Thus, the phenomenon of judging the object as a plane with the ground or wall may occur when the plane is extracted. Thus, the horizontal distance and normal

selected point exceeds the given threshold, the adjacent point will be assigned to a new candidate cluster, and the point is also searched for its adjacent point by complying with the identical strategy. Continue this process until the number of points in the candidate area satisfies the set conditions.

The optimal plane model is extracted from \mathcal{P}_c by Eq. (10). Subsequently, inliers should be assessed. After the initial plane equation is obtained, the other unused points are classified as outer points for the respective subset. To achieve the final plane extraction result, a test should be continued close to the candidate region to verify whether the confidence number of the interior point is sufficient to support the current plane equation. If so, it can be determined as the final trusted plane component.

In algorithm 2, all the algorithms are briefly summarized.

Algorithm 2. Multiplane estimation of improved RANSAC

Input: building components C_v and C_h

Output: plane model $P_{1\dots i}$

1. for $i :=$ each group in Input Data do
2. Starts with a randomly selected point(PC_i)
3. Search for neighbours of (PC_i) with Heuristic search strategy
Calculate the candidate set I_c with Equation (11) and (12)
4. $D_n = \|p \cdot n\|$
5. $D_h = \|\mathbf{p}_i - \mathbf{p}_j\|_2$
6. if $d_i < \Delta d$ and $d_h < \Delta h$
add to I_c
7. end if
8. [$P_1, inlier1$] = $Plane_Fitting(PC_{Candidate})$
9. if $|inlier1| < I_{max}$
10. Search points near P_1
11. if $p_i \in P_1$
Add point to $|inlier1|$
12. end if
13. return P_1
14. $PC_{rest} = Delete(PC\{pc_i|i \in P_1\})$
15. Compute $planeP_2$ with PC_{rest}
16. Repeat until it is impossible to select a feasible plane
from the remaining points
19. return $P_{1\dots i}$

distance are set as the threshold for inliers (Fig. 2). The horizontal distance D_h and the normal distance D_n of two adjacent points $\mathbf{p}_{x_i, y_i, z_i}$ and $\mathbf{p}_{x_j, y_j, z_j}$ are defined as:

$$D_h = \|\mathbf{p}_i - \mathbf{p}_j\|_2 \quad (11)$$

where D_h is the Euclidean distance in the XY coordinate of \mathbf{p}_i and \mathbf{p}_j .

$$D_n = |\mathbf{p}_i \cdot \mathbf{n}_i| \quad (12)$$

where \mathbf{n}_i represents the normal vector of \mathbf{p}_i .

In the first step, a local search heuristic search strategy is adopted to build the set of candidate points \mathcal{P}_c . First, a point is select from the component subset, then its adjacent points are selected, and the search strategy presented in Eqs. (11) and (12) is adopted to determine the horizontal distance D_h and normal distance D_n between the two points. If the $D_h < \Delta h$ and $D_n < \Delta n$, add the points to the candidate cluster as candidate points. If the distance between the adjacent point and the

4. Results

In this experiment, two datasets are used, one of which is four datasets from apartment scans provided by the autonomous system lab of the Swiss Federal Institute of Technology in Zurich (ETH). The other is offered by the Visualization and Multimedia Lab at University of Zurich (UZH). In this experiment, the ceiling is removed to facilitate observation.

4.1. Case study on four indoor environment

The first group is the point cloud data of the hallway, with 370,940 points on the whole. The second is the office point cloud data, which has 364,357 points, which covers a sofa and a table and a chair. Moreover,

the third dataset is office point cloud data, covering a total of 369,095 points. It is noteworthy that in this dataset, the chair is removed and a box is placed against the wall. The fourth group refers to the bathroom point cloud data, which covers 367,732 points, containing a toilet, a bath curtain close, as well as a wash pool. The fifth dataset is the indoor scene data provided by UZH, covering a total of 1,048,565 points.

Figures 3–8 illustrates the extraction results in detail. In the test result figure of the experiment, the ground is marked as red and the wall is marked as blue and yellow. Figure 3 presents the test results of the hallway, Figs. 4–6 presents the plane test results of different scanning angles of office. To be specific, a box is placed on the wall in the environment of Fig. 5. Figure 7 is the detection figure of the bathroom. As can be seen from the result, the main structural planes (e.g., walls, floors, ceilings) in the indoor environment are effectively detected, and the plane point clouds (e.g., lockers) and non-structural target point clouds (e.g., chairs, potted plants) with a point cloud number less than 1000 are removed.

Tables 1–4 list the estimated plane model parameters for the respective scene in the first dataset. Table 1 lists the parameters of five planar models extracted from the Hallway environment. Tables 2 and 3 present the estimated plane model parameters in office environments from different perspectives. Table 4 shows the model parameters of five planes extracted from the bathroom.

4.2. Performance assessment

In this experiment, two assessment methods, *S_Dbw* [34] and Separation(Sp), are selected to assess the validity of the method in this study. *S_Dbw* is a comprehensive assessment index, which properly combines the two criteria of "good" clustering (that is, compactness and separation), so that the clustering results can be reliably evaluated:

$$S_Dbw(c) = Scat(c) + Dens_bw(c) \quad (13)$$

Scat(c) indicates that the average scattering within *c* cluster and can be expressed as:

$$Scat(c) = \frac{1}{c} \sum_{i=1}^c \frac{\|\sigma(v_i)\|}{\|\sigma(S)\|} \quad (14)$$

Where $\sigma(S)$ is the variance of a data set. The term $\sigma(v_i)$ is the variance of cluster c_i .

A smaller value of this metric indicates a compact cluster.

Dens_bw(c) represents the relationship between the average number of points between the *c* clusters in relation with density within the cluster, which is defined as:

$$Dens_bw(c) = \frac{1}{c \cdot (c - 1)} \sum_{i=1}^c \left[\sum_{\substack{j=1 \\ i \neq j}}^c \frac{dens(u_{ij})}{maxdens(v_i), dens(v_j)} \right] \quad (15)$$

where v_i, v_j are centers of clusters c_i, c_j , and the u_{ij} is the midpoint of the line defined by the center of the cluster.

$$dens(u) = \sum_{l=1}^n f(x_l, u), xl \in c_i \cup c_j \subseteq S \quad (16)$$

where n_{ij} represents the number of points in the neighborhood of u . A small value of *Dens_bw(c)* indicates a well-separated cluster. The number of clusters *c* that minimizes the above index can be considered as the best value of the number of clusters that exist in the data set.

The assessment results are shown in Table 5. From the results, it can be seen that the method proposed in this study is better than the conventional RANSAC algorithm in extracting the building plane on indoor point cloud data.

5. Conclusion

For the plane detection on indoor point clouds, a method based on space decomposition and optimized RANSAC is proposed in this study. First of all, before detecting planes in the indoor point cloud, the weighted PCA method is used to estimate the normal vector of the indoor point cloud. Next, angular clustering is adopted to decompose the building components of interior space and obtain the corresponding subset of components (a series of parallel planes in each subset). Lastly, the optimized RANSAC method is used to estimate the main planes of each component, and the final detection result is obtained. The optimized RANSAC extends the conventional RANSAC by considering the pre-aggregated input data and introducing a new threshold constraint. The experimental results show that the method proposed in this study can effectively detect the main planes of indoor environment.

One limitation of the method proposed in this study is that the algorithm is not completely automatic. Including the value of the number of domain points in the weighted PCA algorithm and the thresholds δd and δL in RANSAC are all set manually following the original indoor point cloud obtained. The current and future research will focus on combining the optimized RANSAC algorithm with statistical ideas, and imagine that the median of absolute deviation is exploited to measure the dispersion of the geometric parameters of point cloud data, so that different sets of geometric characteristic elements are divided based on the parameter values for subsequent detection tasks, so the method of this study can be extended to more complex outdoor urban environment and intensive plane detection research.

CRediT authorship contribution statement

Lina Yang: Funding acquisition, Validation, Writing – review & editing. **Yuchen Li:** Investigation, Methodology, Writing – original draft. **Xichun Li:** Validation. **Zuqiang Meng:** Project administration. **Huiwu Luo:** Data curation, Writing – review & editing.

Declaration of Competing Interest

All authors disclosed no relevant relationships.

Acknowledgment

This work is financially supported by the Nature Science Foundation with No. 61862005 and 61762009.

References

- [1] R. Sahba, Sahba, Using a combination of LiDAR, RADAR, and image data for 3D object detection in autonomous vehicles. 2020 11th IEEE Annual Information Technology, Electronics and Mobile Communication Conference (IEMCON), IEEE, 2020, pp. 0427–0431.
- [2] P. Realpe-Muñoz, Collazos, Eye tracking-based behavioral study of users using e-voting systems, Comput. Stand. Interfaces 55 (2018) 182–195.
- [3] C.-P. Chang, J.-C. Lee, Y. Su, P.S. Huang, T.-M. Tu, Using empirical mode decomposition for iris recognition, Comput. Stand. Interfaces 31 (4) (2009) 729–739.
- [4] C. Barba-González, Nebro, Injecting domain knowledge in multi-objective optimization problems: a semantic approach, Comput. Stand. Interfaces 78 (2021) 103546.
- [5] Y. Xie, Tian, Linking points with labels in 3D: a review of point cloud semantic segmentation, IEEE Geosci. Remote Sens. Mag. 8 (4) (2020) 38–59.
- [6] E. Grilli, Menna, A review of point clouds segmentation and classification algorithms, Int. Arch. Photogramm. Remote Sens. Spatial Inf. Sci. 42 (2017) 339.
- [7] S. Mozaffari, O.Y. Al-Jarrah, M. Dianati, P. Jennings, A. Mouzakitis, Deep learning-based vehicle behavior prediction for autonomous driving applications: a review, IEEE Trans. Intell. Transp. Syst. (2020).
- [8] S.-C. Wei, Y.-C. Hou, Y.-C. Lu, A technique for sharing a digital image, Comput. Stand. Interfaces 40 (2015) 53–61.
- [9] H. Park, Kim, Efficient machine learning over encrypted data with non-interactive communication, Comput. Stand. Interfaces 58 (2018) 87–108.
- [10] D.-C. Lou, H.-K. Tso, J.-L. Liu, A copyright protection scheme for digital images using visual cryptography technique, Comput. Stand. Interfaces 29 (1) (2007) 125–131.

- [11] Y. Yu, Y. Zhao, Y. Li, X. Du, L. Wang, M. Guizani, Blockchain-based anonymous authentication with selective revocation for smart industrial applications, *IEEE Trans. Ind. Inf.* 16 (5) (2019) 3290–3300.
- [12] X. Leng, Xiao, A multi-scale plane-detection method based on the hough transform and region growing, *Photogramm. Record* 31 (154) (2016) 166–192.
- [13] A. Khaloo, Lattanzi, Robust normal estimation and region growing segmentation of infrastructure 3D point cloud models, *Adv. Eng. Inf.* 34 (2017) 1–16.
- [14] T. Rabbani, V.D. Heuvel, Segmentation of point clouds using smoothness constraint, *Int. Arch. Photogramm. Remote Sens. Spatial Inf. Sci.* 36 (5) (2006) 248–253.
- [15] H. Son, Kim, Fully automated as-built 3D pipeline extraction method from laser-scanned data based on curvature computation, *J. Comput. Civil Eng.* 29 (4) (2015) B4014003.
- [16] A. Dimitrov, Golparvar-Fard, Segmentation of building point cloud models including detailed architectural/structural features and MEP systems, *Autom. Constr.* 51 (2015) 32–45.
- [17] J. Illingworth, J. Kittler, A survey of the hough transform, 1988.
- [18] X. Leng, Xiao, A multi-scale plane-detection method based on the hough transform and region growing, *Photogramm. Record* 31 (154) (2016) 166–192.
- [19] F.A. Limberger, Real-time detection of planar regions in unorganized point clouds, *Pattern Recognit.* 48 (6) (2015) 2043–2053.
- [20] E. Vera, Lucio, Hough transform for real-time plane detection in depth images, *Pattern Recognit. Lett.* 103 (2018) 8–15.
- [21] C. Mura, Wyss, Robust normal estimation in unstructured 3D point clouds by selective normal space exploration, *Vis. Comput.* 34 (6) (2018) 961–971.
- [22] R. Zhao, Pang, Robust normal estimation for 3D LiDAR point clouds in urban environments, *Sensors* 19 (5) (2019) 1248.
- [23] M.A. Fischler, Bolles, Random sample consensus: a paradigm for model fitting with applications to image analysis and automated cartography, *Commun. ACM* 24 (6) (1981) 381–395.
- [24] F. Tarsha-Kurdi, Landes, Hough-transform and extended RANSAC algorithms for automatic detection of 3D building roof planes from LiDAR data. *ISPRS Workshop on Laser Scanning 2007 and SilviLaser 2007* vol. 36, 2007, pp. 407–412.
- [25] O. Gallo, Manduchi, CC-RANSAC: fitting planes in the presence of multiple surfaces in range data, *Pattern Recognit. Lett.* 32 (3) (2011) 403–410.
- [26] X. Qian, C. Ye, NCC-RANSAC: a fast plane extraction method for 3-D range data segmentation, *IEEE Trans. Cybern.* 44 (12) (2014) 2771–2783.
- [27] Marcelo, Saval-Calvo, Three-dimensional planar model estimation using multi-constraint knowledge based on k-means and RANSAC, *Appl. Soft Comput.* (2015).
- [28] R. Schnabel, Wahl, Efficient RANSAC for point-cloud shape detection. *Computer Graphics Forum* vol. 26, Wiley Online Library, 2007, pp. 214–226.
- [29] S. Yuheng, Y. Hao, Image segmentation algorithms overview, *arXiv preprint arXiv: 1707.02051* (2017).
- [30] A. Ebrahimi, S. Czarnuch, Automatic super-surface removal in complex 3D indoor environments using iterative region-based RANSAC, *Sensors* 21 (11) (2021) 3724.
- [31] J. Straub, Freifeld, The manhattan frame model–manhattan world inference in the space of surface normals, *IEEE Trans. Pattern Anal. Mach. Intell.* 40 (1) (2017) 235–249.
- [32] H. Hoppe, DeRose, Surface reconstruction from unorganized points. *Proceedings of the 19th Annual Conference on Computer Graphics and Interactive Techniques*, 1992, pp. 71–78.
- [33] J. Sanchez, Denis, Robust normal vector estimation in 3D point clouds through iterative principal component analysis, *ISPRS J. Photogramm. Remote Sens.* 163 (2020) 18–35.
- [34] M. Halkidi, Vazirgiannis, Clustering validity assessment: finding the optimal partitioning of a data set. *Proceedings 2001 IEEE International Conference on Data Mining*, IEEE, 2001, pp. 187–194.